

3D Deconvolution with Deep Learning

Abhijeet Phatak^{1,2} (aphatak@stanford.edu)

Solgaard Lab¹, Department of Electrical Engineering², 350 Serra Mall, Stanford University.



Motivation

- 3D Deconvolution is a typical problem faced by microscopists and astronomers which aims at reverse the effects of convolution on observed data .
- Computational complexity and not precisely known noise parameters (Gaussian, Poisson, Optical aberrations) make it challenging.
- Typically the three major categories of deconvolution algorithms are: Non-iterative (Wiener filtering), Iterative (RL, ADMM) and blind deconvolution.
- Changing certain microscopy parameters may change the point spread function (PSF) which requires recalibration. Sometimes, it is not trivial to model the image formation process because of complex optical setup.
- To circumvent these issues, we focus on using deep learning (Convolutional Neural Networks) for 3D deconvolution by efficiently learning the underlying ground truth from the blurred data.
- We also compare the results to standard methods like RL and ADMM.

References

- Varma, Paroma, and Gordon Wetzstein. "Efficient 3D Deconvolution Microscopy with Proximal Algorithms." *Imaging Systems and Applications*. Optical Society of America, 2016.
 - Dong, Chao, et al. "Image super-resolution using deep convolutional networks." *IEEE transactions on pattern analysis and machine intelligence* 38.2 (2016): 295-307.
 - Weigert, Martin, et al. "Isotropic reconstruction of 3D fluorescence microscopy images using convolutional neural networks." *International Conference on Medical Image Computing and Computer-Assisted Intervention*. Springer, Cham, 2017.
 - Weigert, Martin, et al. "Content-Aware Image Restoration: Pushing the Limits of Fluorescence Microscopy." *bioRxiv* (2017): 236463.
1. <http://www.cellimagelibrary.org/images/36797>

Methods

Richardson Lucy (RL) Deconvolution^[1]

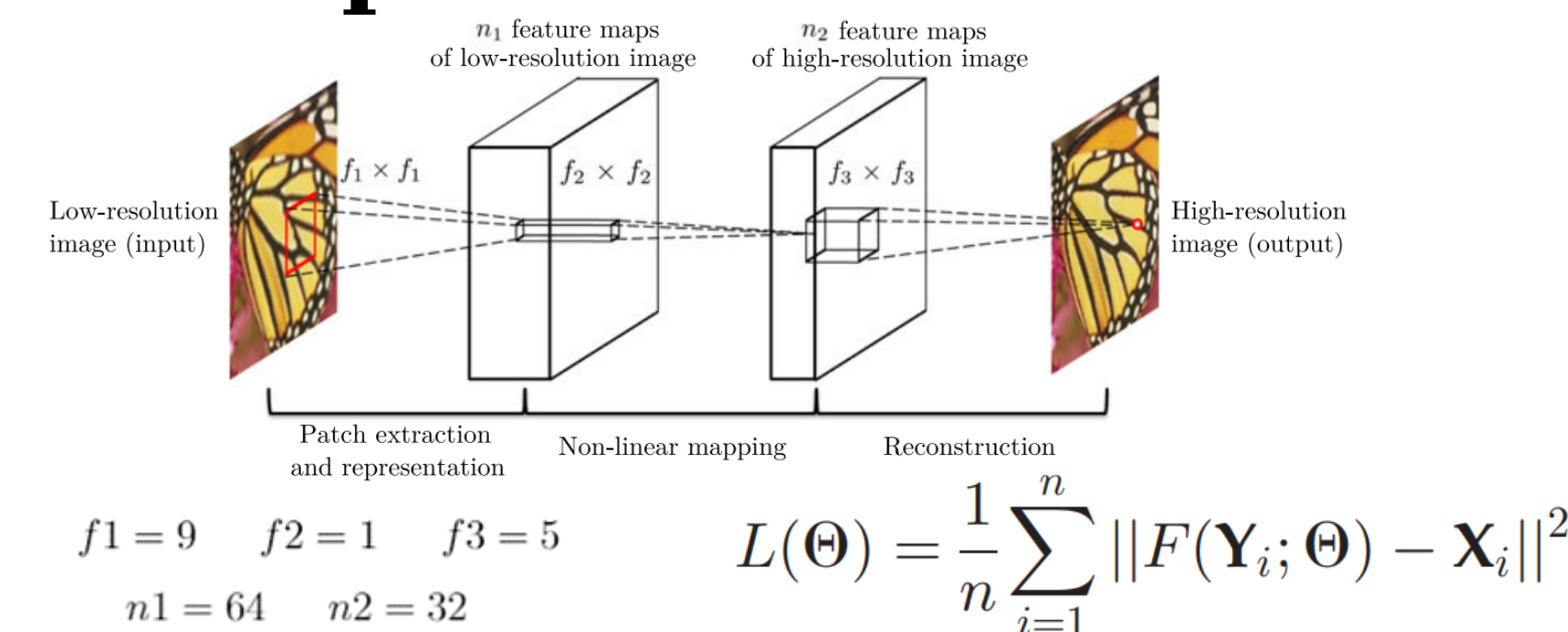
$$\mathbf{b} \sim P(\mathbf{Ax})$$
$$\mathbf{x}^{(q+1)} = \frac{\mathbf{A}^T \left(\frac{\mathbf{b}}{\mathbf{Ax}} \right)}{\mathbf{A}^T \mathbf{1} - \lambda \left(\frac{\mathbf{D}_{xx}}{|\mathbf{D}_{xx}|} + \frac{\mathbf{D}_{yx}}{|\mathbf{D}_{yx}|} + \frac{\mathbf{D}_{zx}}{|\mathbf{D}_{zx}|} \right)} \mathbf{x}^{(q)}$$

ADMM Deconvolution^[1]

$$\begin{aligned} & \underset{\mathbf{x}}{\text{minimize}} \quad \sum_i g_i(\mathbf{z}_i) \\ & = g_1(\mathbf{z}_1) + g_2(\mathbf{z}_2) + g_3(\mathbf{z}_3) \\ & \text{subject to} \quad \underbrace{\begin{bmatrix} \mathbf{A}^T & \mathbf{I}^T & \mathbf{D}^T \end{bmatrix}^T}_{\mathbf{K}} \mathbf{x} \\ & \quad = \underbrace{\begin{bmatrix} \mathbf{z}_1^T & \mathbf{z}_2^T & \mathbf{z}_3^T \end{bmatrix}^T}_{\mathbf{z}} \end{aligned}$$

Initialization: $\mathbf{x}_{init} = \mathbf{b}, \mathbf{v} = \mathbf{z} = \mathbf{u} = 0, \rho > 0$
for $k = 1$ to MaxIter
 $\mathbf{x} \leftarrow \text{prox}_{\text{quad}}(\mathbf{v}), \mathbf{v} = \mathbf{z} - \mathbf{u}$
 $\mathbf{z} \leftarrow \text{prox}_{g_i, \rho}(\mathbf{v}), \mathbf{v} = \mathbf{Kx} + \mathbf{u}$
 $\mathbf{u} \leftarrow \mathbf{u} + \mathbf{Kx} - \mathbf{z}$
end

Naïve Super-Resolution CNN^[2]



Isonet-1^[3,4]

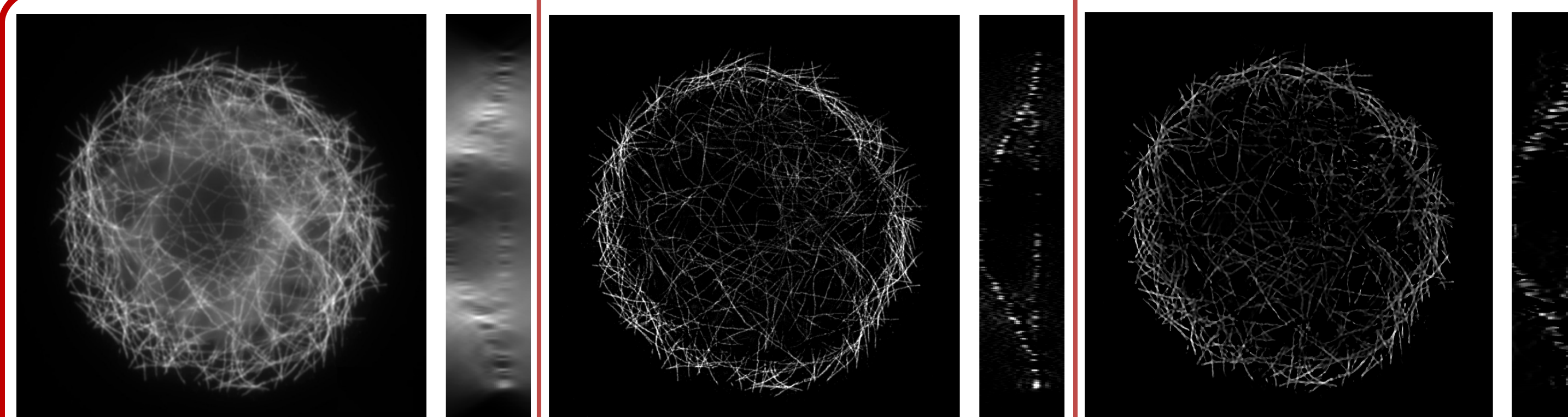
$$g = \mathcal{P}[\mathcal{S}_\sigma(h \otimes f)] + \eta \quad p_{xy} = \mathcal{S}_\sigma(\tilde{h} \otimes g_{xy})$$

$$C_{64,9,9} - C_{32,5,5} - C_{1,5,5} - C_{1,1,1}$$

$$\mathcal{L} = \sum_n -[20 \log_{10} \max g_{xy,n} - 10 \log_{10} |g_{xy,n} - \tilde{g}_{xy,n}|^2]$$

Drosophila S2 cell 3D dataset available publicly^[4]. Spatially varying 3D PSF was estimated with inverse filtering technique with the widefield image taken as the blurred image (b) and the structure illumination image as the ground truth (x). Validated with PSF from deconvblind (MATLAB)

Results and Discussion



(x,y) and (x,z) sections of Widefield, Ground Truth, Deconvolved Images

RL – Performs reasonably well when there is Poisson Noise

ADMM – Faster convergence than RL but still we need to know the image formation process explicitly.

Naïve SRCNN – Ignores PSF and hence performs poorly

Isonet1 – Restores isotropic resolution by solving a super-resolution problem on subsampled data, and a deconvolution problem to correct for the PSF.

Detailed analysis of convergence and PSNR is available in the final report.

| Method | PSNR | Time(s) |
|----------|--------|---------|
| RL | 20.842 | 326 |
| ADMM | 22.151 | 418 |
| SRCNN | 18.192 | 303 |
| Isonet-1 | 23.151 | 780 |